Revisiting the Integral Charge Control Relation (ICCR)

1. Antecedents

Different base resistance values have been obtained for the VM (VBIC-MEXTRAM) and Hicum based models by performing the extraction from high-frequency two-port parameters with a novel method described in [14]. Particularly, computing the base resistance from the expression

$$(1+cf)\cdot rbi + cf\cdot rci + re = \frac{\Im(\tilde{h}_{21}\,conj(\tilde{h}_{11}))}{\Im(\tilde{h}_{21})}$$

one finds

$$\boxed{rbi_{Hicum} > rbi_{VM}}$$

The $\tilde{h}$ parameters denote measurement data deembedded from the external parasitic resistances *rbx* and *rcx* and modified by removing the external collector capacitance. Parameter *cf* is a correction factor determined by the internal collector capacitance *cjci*, the intrinsic transconductance *gm* and transit frequency ω_T of the device. The rest of the notations have their usual meanings.

Clearly the internal collector resistance *rci* what exists in VM but is zero in the present Hicum equivalent must play a key role in the paradox. Since apparently every other parameter must have the same values the root of the discrepancy has been suspected to be related to the fundaments of the model concepts.

Without going into the details of compact model formulas the basic starting point of all present bipolar models, the integral charge control principle of H. K. Gummel has been revisited with respect to its application at the various model families.

2. Some Basic Semiconductor Equations

Poisson's Equation

The electrostatic potential ψ satisfies the second order d.e.

$$\frac{d^2\psi}{dx^2} = -\frac{q}{\varepsilon_{si}}\left[p(x) - n(x) + N_d(x) - N_a(x)\right] \tag{1}$$

Definition of the Quasi-Fermi Potentials

$$\varphi_n = \psi - V_T \ln\left(\frac{n}{n_i}\right) \tag{2n}$$

$$\varphi_p = \psi + V_T \ln\left(\frac{p}{n_i}\right) \tag{2p}$$

It follows

$$n = n_i \exp\left(\frac{\psi - \varphi_n}{V_T}\right) \tag{3n}$$

$$p = n_i \exp\left(\frac{\varphi_p - \psi}{V_T}\right) \tag{3p}$$

and

zoltan.huszka@austriamicrosystems.com

$$n \cdot p = n_i^2 \exp\left(\frac{\varphi_p - \varphi_n}{V_T}\right) \tag{4}$$

Currents

$$J_n = -q\mu_n n \frac{d\varphi_n}{dx} \tag{5n}$$

$$J_p = -q\mu_p p \frac{d\varphi_p}{dx} \tag{5p}$$

3. The Transistor Structure

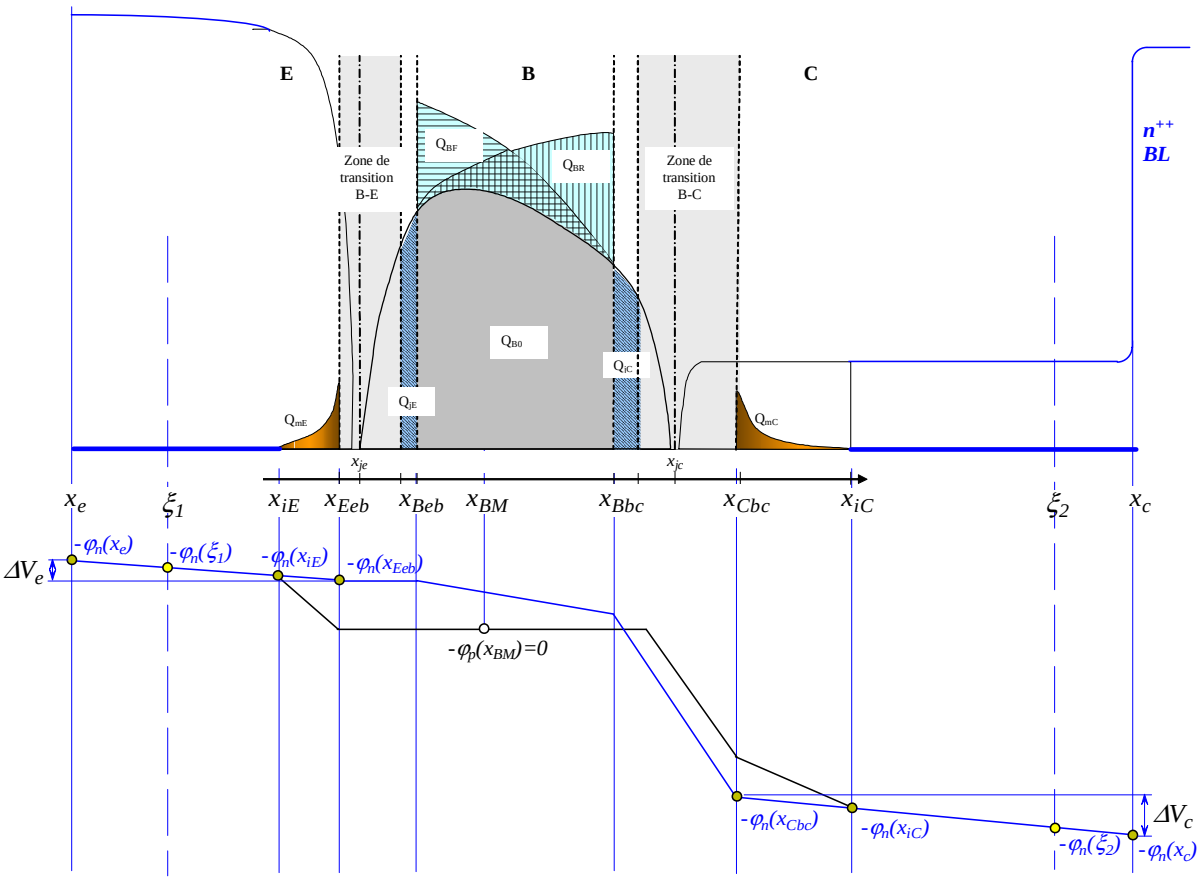

Fig. 1 Doping, charge distribution and energy diagram of an *npn* transistor at reverse collector bias. Collector charge Q_{mC} is present at (quasi)saturation.
(core of the upper semi-figure: courtesy of B. Ardouin, XMOD)

The one-dimensional transistor takes place within the emitter contact x_e and the collector contact x_c as shown on Fig. 1. The former is the boundary between the polycrystalline and the monocrystalline emitter, the latter is the edge of the highly doped buried layer. The electron and hole quasi-Fermi levels φ_n and φ_p respectively are sketched under the doping profile and charge distribution plots on an inverted scale.
The normal active mode of operation is shown where the *EB* junction is forward-, the (internal) *CB* junction is reverse biased. Minority charge Q_{mE} is always present in the emitter under normal operating conditions while Q_{mC} develops e.g. at quasi or deep saturation. The injection– or neutrality - points in the emitter x_{iE} and the collector x_{iC} are the locations where the electron and hole quasi-Fermi potentials collapse.

zoltan.huszka@austriamicrosystems.com

4. The ICCR Principle

In an *npn* transistor the transfer current J_T is carried by electrons throughout the whole structure. The base current is separately discussed in the particular modelling details but as the relative loss of J_T is small it is neglected in the ICCR formulation.
From (5n) and (4)

$$-J_n = J_T = q\mu_n n \frac{d\varphi_n}{dx}$$

$$J_T \frac{1}{\mu_n n} = qV_T \frac{d}{dx}\left(\frac{\varphi_n}{V_T}\right)$$

4.1 *"Modern" treatment*

$$J_T \frac{p}{\mu_n \cdot p \cdot n} = qV_T \frac{d}{dx}\left(\frac{\varphi_n}{V_T}\right)$$

Substituting (4) for the $n\cdot p$ product

$$J_T \frac{p \exp\left(\frac{-\varphi_p + \varphi_n}{V_T}\right)}{\mu_n n_i^2} = qV_T \frac{d}{dx}\left(\frac{\varphi_n}{V_T}\right) \tag{6}$$

Rearranging

$$J_T \frac{p \exp\left(\frac{-\varphi_p}{V_T}\right)}{n_i^2 \cdot \mu_n} = -qV_T \frac{d}{dx}\left[\exp\left(\frac{-\varphi_n}{V_T}\right)\right] \tag{7}$$

This equation is valid anywhere between the emitter and collector contacts. Integrating both sides between two abscissae ξ_1 and ξ_2 such that

$$\xi_1, \xi_2 \in [x_e, x_c] \tag{8}$$

we get

$$J_T \int_{\xi_1}^{\xi_2} \frac{p \exp\left(\frac{-\varphi_p}{V_T}\right)}{n_i^2 \cdot \mu_n} dx = qV_T \left[\exp\left(\frac{-\varphi_n(\xi_1)}{V_T}\right) - \exp\left(\frac{-\varphi_n(\xi_2)}{V_T}\right)\right] \tag{9}$$

The potential reference can be arbitrarily selected. A convenient choice is the hole quasi-Fermi potential in the middle point x_{BM} of the metallurgical EB and BC junctions because φ_p is constant throughout the base region:

$$\varphi_p(x_{BM}) = 0 \tag{10}$$

The integral on the LHS is the Gummel number of the volume between the integration boundaries

$$G(\xi_1, \xi_2) = \int_{\xi_1}^{\xi_2} \frac{p \exp\left(\frac{-\varphi_p}{V_T}\right)}{n_i^2 \cdot \mu_n} dx \tag{11}$$

The partitioning the Gummel number will not be detailed here. Substitution in (9) yields

$$\boxed{J_T = qV_T \frac{\exp\left(\frac{-\varphi_n(\xi_1)}{V_T}\right) - \exp\left(\frac{-\varphi_n(\xi_2)}{V_T}\right)}{G(\xi_1, \xi_2)}} \tag{12}$$

zoltan.huszka@austriamicrosystems.com

This is the ICCR principle.

The current is invariant against the selection of the integration boundaries until condition (8) is satisfied. The various model concepts basically differ in the specific definition of these integration limits.

It can be observed on Fig. 1 that in the region bounded by the external sides of the space charge layers $[x_{Eeb},x_{Cbc}]$ the hole quasi-Fermi level is practically constant. With the reference selection (10) the exponential term in the integrand of (11) can be omitted. The Gummel number here can be computed as the hole charge weighted by the position dependent denominator. The effect of heterojunctions can be taken into account through the intrinsic concentration n_i.

In the injection regions φ_p is not constant any more and the Gummel number in these intervals has to be computed by special considerations. These details do not affect the generality of this discussion and will not be dealt with here.

4.2 *"Classical" treatment (Gummel70 [1])*

In the original publication [1] on the ICCR a *pnp* transistor was investigated. The analysis below will be made on *npn* transistors with a few minor changes not affecting the results of the referred paper. Gummel assumed an electric field dependent mobility in the form of

$$\frac{1}{\mu}=\frac{1}{\mu_0}+\frac{|E|}{v_s}=\frac{V_T}{D_0}+\frac{1}{v_s}\left|\frac{d\psi}{dx}\right|$$

The factor on the LHS of (7) converts with

$$p\exp\left(\frac{-\varphi_p}{V_T}\right)=n_i\exp\left(\frac{-\psi}{V_T}\right)$$

to

$$V_T\frac{p\exp\left(\frac{-\varphi_p}{V_T}\right)}{n_i^2}\frac{1}{V_T\cdot\mu_n}=V_T\left[\frac{n_i\exp\left(\frac{-\psi}{V_T}\right)}{n_i^2 D_n}+\frac{\exp\left(\frac{-\psi}{V_T}\right)}{n_i\cdot v_s}\left|\frac{d}{dx}\left(-\frac{\psi}{V_T}\right)\right|\right]$$

$$V_T\frac{p\exp\left(\frac{-\varphi_p}{V_T}\right)}{n_i^2}\frac{1}{V_T\cdot\mu_n}=V_T\left[\frac{\exp\left(\frac{-\psi}{V_T}\right)}{n_i D_n}+\frac{1}{n_i\cdot v_s}\left|\frac{d}{dx}\left(\exp\left(\frac{-\psi}{V_T}\right)\right)\right|\right]$$

The diffusion constant D_n in these expressions is the - doping dependent - low field value.

The electrostatic potential takes its (negative) extremum in the *p* base at x_{BM} with a value of ψ_m. The major contribution to the integral between the metallurgical junctions $[x_{je},x_{jc}]$ comes dominantly from the part close to ψ_m thus for the first term – the Gummel number – the following unequality holds

$$G(x_{je},x_{jc})<w_B\left[\frac{V_T}{\overline{n}_i\cdot\overline{D}_n}\exp\left(\frac{-\psi_m}{V_T}\right)\right]$$

The integral of the second, field-dependent term is performed separately in the intervals $[x_{je},x_{BM}]$ and $[x_{BM},x_{jc}]$ to resolve the absolute value function. The exponentials at the junctions are negligible compared to the value at the potential minimum thus

$$G_E(x_{je},x_{jc})\approx\frac{2\overline{D}_n}{v_s}\left[\frac{V_T}{\overline{n}_i\cdot\overline{D}_n}\exp\left(\frac{-\psi_m}{V_T}\right)\right]$$

zoltan.huszka@austriamicrosystems.com

With round values of $v_s = 1 \cdot 10^7 cm/s$ and $D_n = 10 cm^2/s$ we have $\frac{2\overline{D}_n}{v_s} \approx 20nm$. In 1970 when Gummel wrote his paper this was negligible compared to the contemporary base widths. Today however the metallurgical base width even for a moderate frequency transistor of f_T=50GHz is w_B=28nm [2].

At modern high frequency transistors the contribution of the mobility field dependent base charge term is comparable to the base-Gummel number and must be taken into account.

5. Bipolar Transistor Model Categories

5.1. Regional Approach (Getreu, 1978 [3])

In his book "Modelling the Bipolar Transistor" 1978 [3], Getreu located the integration boundaries to the emitter side of the EB and the collector side of the BC space charge layers. As opposed to the original model formulation of Gummel and Poon [4] with the boundaries at the emitter and collector contacts, he noted that this way `"... no assumption is made about the minority carrier quasi-Fermi levels in the neutral emitter and collector regions ..."`. (It is interesting to recall that Gummel applied also these boundaries when formulating the ICCR [1]. It is a mystery why did he change his mind half a years later in [4])

The transfer current with $\xi_1 = x_{Eeb}$ and $\xi_2 = x_{Cbc}$ becomes

$$J_T = qV_T \frac{\exp\left(\frac{V_{Beb,Eeb}}{V_T}\right) - \exp\left(\frac{V_{Bbc,Cbc}}{V_T}\right)}{G(x_{Eeb}, x_{Cbc})} \tag{13}$$

The arguments in the numerator with the potential reference selection (10) are the *biases across the two space charge layers* as seen on the quasi-Fermi level diagram. The junction voltages directly determine the minority carrier concentrations at the depletion layer edges through the Boltzmann relation. Consequently the Gummel number in the denominator is also determined as a function of this pair of bias voltages.

$V_{Beb,Eeb}$ and $V_{Bbc,Cbc}$ are the two independent control voltages of the transistor generating the transfer current explicitly through (13).

By this move Getreu not only created a fully measurement-consistent concept but opened the way for the development of a successful model series SGP-VBIC-MEXTRAM with increasing perfection in the regional collector description.

The ΔV_c-J_T relationship in the epilayer - within the interval $[x_{Cbc}, x_c]$ - is analyzed in DC mode on the basis of the extended Kull-Nagel theory with the proper boundary conditions at x_{Cbc}. In other words a bias-point dependent variable internal collector resistance is linked to the model. The AC behaviour is appropriately adjusted by the stored charge in the epilayer. All possible cases i.e. the total depletion, depletion+ohmic, injection+ohmic and injection+hot carrier are considered both in DC and AC.

Mextram has a more refined collector model than VBIC. SGP regards the whole region from x_{Cbc} to the external collector contact – not shown on Fig. 1. - a single constant collector resistance *rc*. In VBIC and MEXTRAM an additional external collector resistance *rcx* represents the fixed ohmic region between x_c and the external collector contact.

zoltan.huszka@austriamicrosystems.com

5.2. Global Approach (Gummel-Poon70 [4], Schroeter-Rein86 [5], Stübing-Rein87 [6])

In this approach the whole transistor is included in the charge control integral by taking the integration boundaries at the position of the emitter x_e and collector x_c contacts. The fixed ohmic regions from these points to the physical contacts can be represented by additional external resistances in the model schematic like in the regional approach.
The transfer current becomes

$$J_T = qV_T \frac{\exp\left(\frac{V_{Beb,e}}{V_T}\right) - \exp\left(\frac{V_{Bbc,c}}{V_T}\right)}{G(x_e, x_c)} \tag{14}$$

This concept was suggested – implicitly though - in the original GP model formulation by Gummel and Poon [4]. However the actual GP models adopted the regional approach of Getreu [3] and the idea was not realized until the introduction of Hicum [5], [6].
Inserting the voltage drops across the crystalline emitter and the epitaxial collector layers from Fig. 1 to (14)

$$J_T = qV_T \frac{\exp\left(\frac{V_{Beb,Eeb}}{V_T} + \frac{\Delta V_e(J_T)}{V_T}\right) - \exp\left(\frac{V_{Bbc,Cbc}}{V_T} - \frac{\Delta V_c(J_T)}{V_T}\right)}{G(x_e, x_c)} \tag{15}$$

$V_{Beb,e}$ and $V_{Bbc,c}$ are not independent control voltages any more because ΔV_e and ΔV_c depend on the transfer current. To preserve an explicit expression for J_T these voltage drops must be neglected.

In the active mode of operation the collector is reverse biased and the second exponential can be omitted. Due to the high conductivity of the recrystallized emitter region the voltage drop ΔV_e across [x_e, x_{Eeb}] is negligible. Hence in normal active mode with reverse internal collector bias (15) is re-formulated in Hicum as

$$\boxed{J_T = qV_T \frac{\exp\left(\frac{V_{Beb,e}}{V_T}\right)}{G(x_e, x_c)} \approx qV_T \frac{\exp\left(\frac{V_{Beb,Eeb}}{V_T}\right)}{G(x_e, x_c)}} \tag{16}$$

The Gummel number is computed regionally across [x_e, x_{Eeb}], [x_{Eeb}, x_{Beb}], [x_{Beb}, x_{Bcb}], [x_{Bcb}, x_{Ccb}] and [x_{Ccb}, x_c] respectively:

$$\boxed{G(x_e, x_c) = G(x_e, x_{Eeb}) + G(x_{Eeb}, x_{Beb}) + G(x_{Beb}, x_{Bbc}) + G(x_{Bbc}, x_{Ccbc}) + G(x_{Cbc}, x_c)} \tag{17}$$

Performing the computations according to (11) the effect of bandgap variations can be considered through the bandgap dependence of the intrinsic concentration n_i. This way HBTs can also be modelled.

The pair of relations (16) and (17) are termed GICCR i.e. the generalized ICCR (Schroeter-Friedriech-Rein93 [7]).

The outstanding innovation of Hicum is to extract the Gummel number (total charge of the carriers interacting with the base terminal) from the measured transit time(s) of the transistor. The fundamental concept of the model is that the transfer current automatically results by substituting the Gummel number - extracted from the transit times – into (16). This is opposite to the regional approach where the DC behaviour has the priority. At high speed circuits the accurate modelling of the AC behaviour may be particularly important hence Hicum is claimed to be more suited for such applications.
The extraction concept provides a superior transit frequency description compared to other existing models.

Omitting ΔV_c i.e. regarding the internal collector resistance zero however is not fully straightforward. The assumption of *rci=0* can introduce errors in the description of both of the DC and AC behavior.

6. Potential Consequences of Neglecting *rci*

6.1 Effect on the DC behavior

The publication of *Stübing-Rein87* [6] what is a comprehensive introduction to the one-dimensional Hicum, limits the applicability of the model in its equation (1) to

$$V_{ce} \geq 0.25V \tag{18}$$

There was no explanation given for the restriction but the reason can be understood from the discussion below.

The validity of the ICCR equation (13) follows not only from the strict theoretical derivation of Gummel [1] but was confirmed numerically as well in [8] and was found to be a fairly good approximation far into the high current region. It follows from (13) that at the condition $V_{Beb,Eeb} = V_{Bbc,Cbc}$ i.e. when the internal collector-emitter voltage is zero $V_{cei} = 0$ the transfer current goes also zero $J_T=0$.

Neglecting ΔV_e the transfer current of the Hicum approach (15) can be re-written as

$$J_{T\_Hicum} = qV_T \frac{\exp\left(\frac{V_{Beb,Eeb}}{V_T}\right)}{G(x_e, x_c)}\left[1 - \exp\left(-\frac{V_{cei} + \Delta V_c(J_T)}{V_T}\right)\right] \tag{19}$$

Hence at $V_{cei} = 0$ Hicum provides a nonzero (positive) transfer current thus

$$\boxed{J_{T\_Hicum} > J_T} \tag{20}$$

Hicum overestimates the transfer current in the quasi/deep saturation regime.

The error can be limited by the condition

$$V_{ce} >> \Delta V_c(J_T) \tag{21}$$

Note that (18), (21) or a similar explicit restriction is missing from the present Hicum documentation [9] in spite of the fact that the fundamental model axioms (16) and (17) have not changed in the meantime.

6.2 Effects on the AC behaviour

6.2.1 Collector time constant

Equation (2) in *Stübing-Rein87* [6] – see also equation (5) in *Schroeter-Rein85* [10] - introduces a modified transit time

$$\tau_f^* = \tau_f + rci \cdot cjci \tag{22}$$

for taking into account the effect of the omitted internal collector resistance on the stored charge. The explicit observation of the collector time constant however can not be found in the recent model equations [9], [11].

Since both *rci* and *cjci* are built on the same cross section, the collector time constant is independent of the lateral device sizes in the first order:

$$\tau_{ci} = rci \cdot cjci = \frac{\varepsilon\varepsilon_0}{q\mu_n N_D}\left(\frac{W_{epi}}{W_d} - 1\right) \tag{23}$$

zoltan.huszka@austriamicrosystems.com

where for simplicity the depletion width W_d is assumed to take place entirely in the collector epi $W_d = \sqrt{\frac{\varepsilon\varepsilon_0 (V_{Cbc,Bbc} + V_B)}{qN_D}}$.

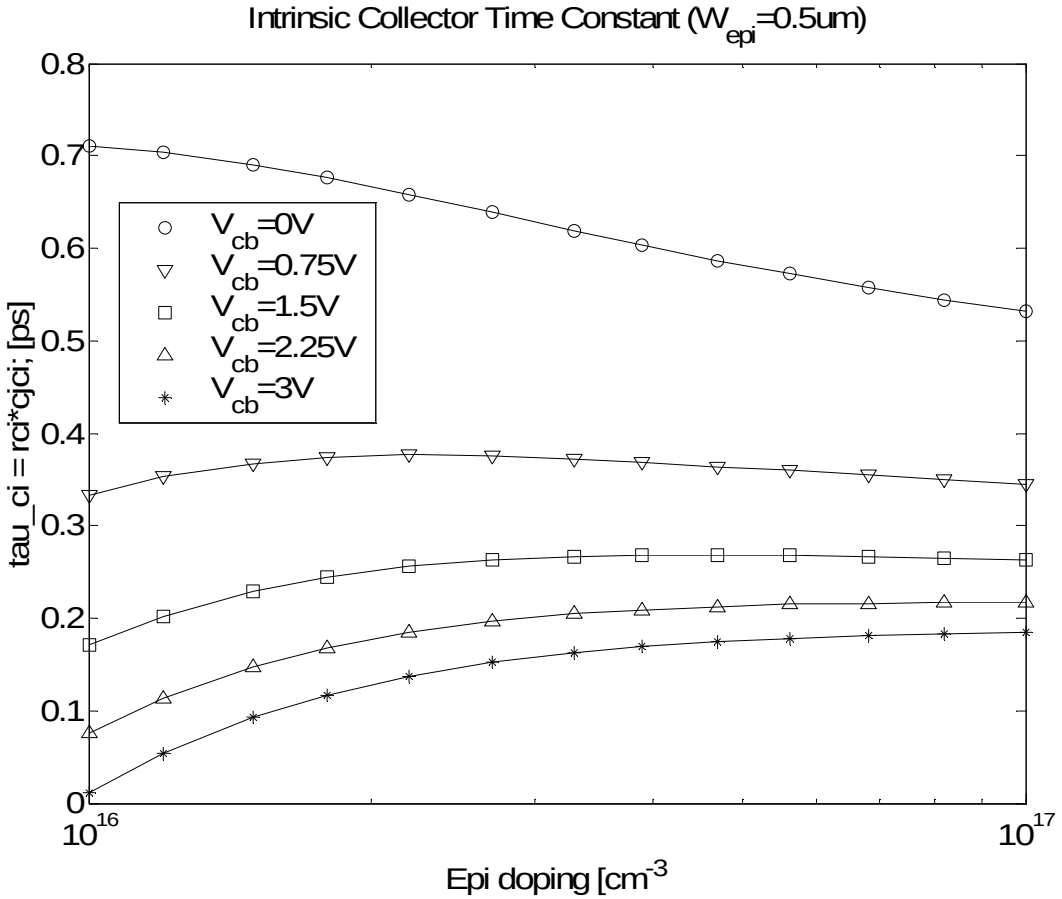

Fig. 2 Collector time constant

Fig. 2 shows τ_{ci} for an epi width of *0.5um* in the range of typical dopings. At an f_T*=150GHz* transistor described in [12] the low bias transit time was found to be *0.68ps*. At modern devices the collector time constant is comparable to the total transit time and must be taken into account.

The low-current transit time component τ_{f0} is described in Hicum [9] by

$$\tau_{f0}(v_{B'C'}) = \tau_0 + \Delta\tau_{0h}(c-1) + \tau_{Bvl}\left(\frac{1}{c} - 1\right) \tag{24}$$

with the normalized internal BC depletion capacitance $1/c = C_{jCi,t}(V_{B'C'})/C_{jCi0}$. Now (23) can be re-written as

$$\tau_{ci} = \frac{\tau_{ci1}}{c} - \tau_{ci0} \tag{25}$$

Though the physical background of τ_{Bvl} is different – carrier jam in the BC space charge layer- the description of τ_{ci} formally can be understood in the present transit time model of Hicum.

The fact of including τ_{ci} in the transit time formulation should be explicitly stated in the model documentation.

zoltan.huszka@austriamicrosystems.com

6.2.2 Two-port parameters

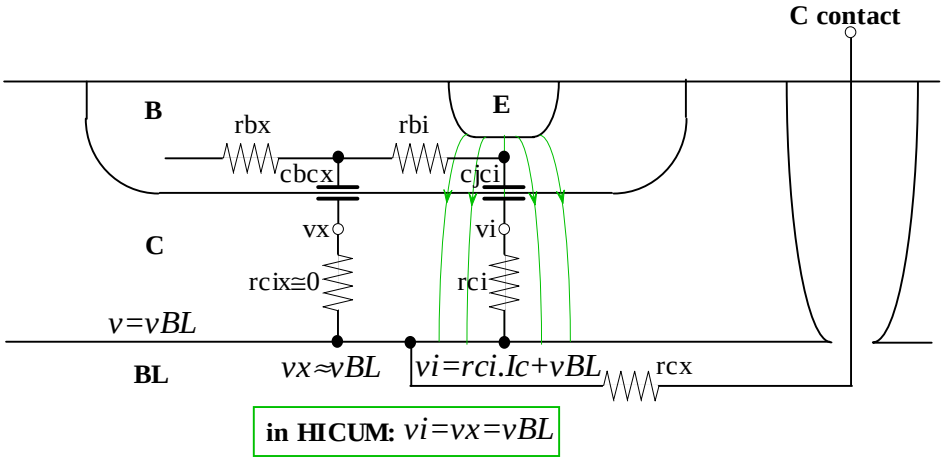

Fig. 3 The Hicum approximation

An intuitive picture of the Hicum approximation is shown on Fig. 3.
The vertical resistance *rcix* to the collector side of the BC junction is less than *rci* under the emitter. Actually it is regarded zero in all models. Assume normal active operation when the collector side of the BC space charge layer is "far" from the BL. Obviously, voltage *vi* at the node of *cjci* is different from *vx* on *cbcx*. Hicum assumes *vi=vx* and both equal to the potential *vBL* at the BL boundary. Network elements *cbcx*, *cjci* and *rcx* meet in one single node removing hereby a physically existing network element from the equivalent. Additionally the DC bias of the two capacitances is forced to be equal what - especially at increasing collector currents - not the case is.
Hicum users might think at the first glance that parameter *rci0* resolves the problem. However *rci0* is a transit time parameter what has an influence on the charge – the denominator of (15) – only. The voltage conditions - numerator of (15) – are not affected by this parameter.
The effect of omitting *rci* on the two-port hybrid parameters will be investigated on the core models of Fig. 4.

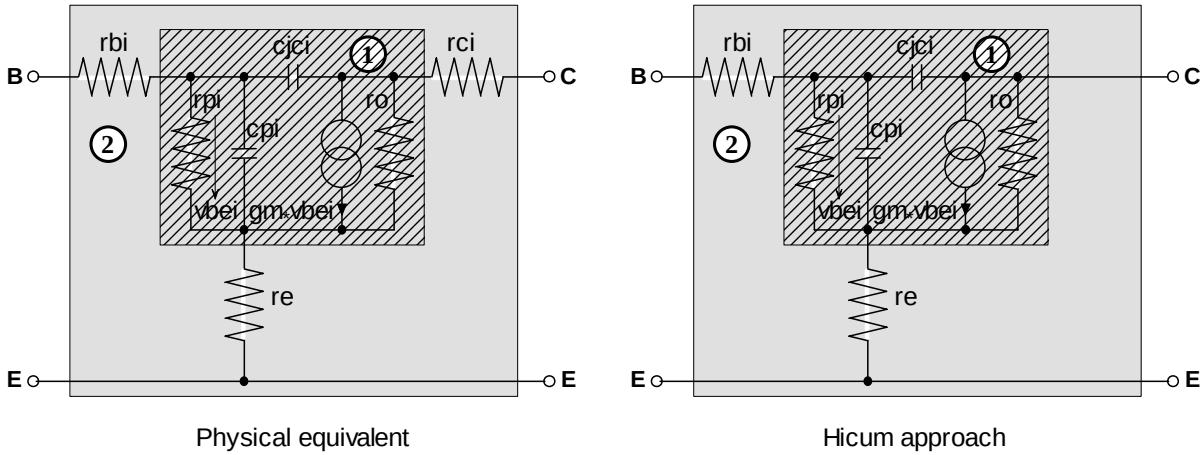

Fig. 4. Simplified Two-Port Equivalents

$$\mathbf{Y}_e^{(1)} = \begin{bmatrix} gpi + s(cpi + cjc) & -s \cdot cjc \\ gm - s \cdot cjc & go + s \cdot cjc \end{bmatrix} \qquad \mathbf{Z}_e^{(2)} = \begin{bmatrix} z_{11e}^{(1)} + rbi + re & z_{12e}^{(1)} + re \\ z_{21e}^{(1)} + re & z_{22e}^{(1)} + rci + re \end{bmatrix}$$

The following identities will be applyed to network#2:

$$h_{11} = z_{11} + h_{21} z_{12} \qquad z_{11} = h_{11} - h_{21} z_{12}$$

Denoting the circuit blocks in the superscripts

$h_{11e}^{(2)} = rbi + re + z_{11e}^{(1)} + h_{21e}^{(2)}(z_{12e}^{(1)} + re) = rbi + re + (h_{11e}^{(1)} - h_{21e}^{(1)} z_{12e}^{(1)}) + h_{21e}^{(2)}(z_{12e}^{(1)} + re)$

Substituting

$$h_{11e}^{(1)} = \frac{h_{21e}^{(1)}}{y_{21e}^{(1)}}$$

we have

$$h_{11e}^{(2)} = rbi + re + h_{21e}^{(2)}(z_{12e}^{(1)} + re) + \frac{h_{21e}^{(1)}}{y_{21e}^{(1)}}$$

It will be assumed that the current gain of network#2 can be equally set to the measurement value $h_{21e}^{(2)} = H_{21e}^{(2)}$ both in the left and in the right (Hicum) model. Quantities referring to the Hicum approach will be subscripted accordingly.

The difference of the input hybrid parameters becomes

$$h_{11e}^{(2)} - h_{11e\_Hicum}^{(2)} = \frac{1}{y_{21e}^{(1)}}(h_{21e}^{(1)} - h_{21e\_Hicum}^{(1)}) \tag{26}$$

The current gain of network#1 can be deduced from

$$h_{21e}^{(2)} = -\frac{z_{21e}^{(1)} + re}{z_{22e}^{(1)} + rci + re}$$

through

$$1 + h_{21e}^{(2)} = \frac{1 + h_{21e}^{(1)} + \dfrac{rci}{z_{22e}^{(1)}}}{1 + \dfrac{rci + re}{z_{22e}^{(1)}}}$$

as

$$1 + h_{21e}^{(1)} = (1 + H_{21e}^{(2)})\left(1 + \frac{rci + re}{z_{22e}^{(1)}}\right) - \frac{rci}{z_{22e}^{(1)}}$$

The difference of the two approaches becomes

$$h_{21e}^{(1)} - h_{21e\_Hicum}^{(1)} = H_{21e}^{(2)} \frac{rci}{z_{22e}^{(1)}}$$

Expressing the output impedance with the admittance parameters and neglecting *go* from $y_{22e}^{(1)}$ we get from (26)

$$h_{11e}^{(2)} - h_{11e\_Hicum}^{(2)} = H_{21e}^{(2)}\left(\frac{y_{22e}^{(1)}}{y_{21e}^{(1)}} - \frac{y_{12e}^{(1)}}{y_{11e}^{(1)}}\right) rci \approx H_{21e}^{(2)}\left(\frac{1}{y_{21e}^{(1)}} + \frac{1}{y_{11e}^{(1)}}\right) s \cdot cjci \cdot rci$$

Above the beta breakpoint frequency

$$\frac{1}{h_{21e}} = \frac{1}{h_{21e0}} + \frac{s}{\omega_T} \approx \frac{s}{\omega_T}$$

Hence the relative deviation of the input hybrid parameters results as

$$\boxed{\frac{h_{11e}^{(2)} - h_{11e\_Hicum}^{(2)}}{h_{11e}^{(1)}} \approx 2\pi \cdot f_T \cdot \tau_{ci}} \tag{27}$$

Reading $\tau_{ci} = 0.5ps$ from Fig. 2, the relative deviation of h_{11e} at f_{Ti}=*50GHz* and *100GHz* respectively is *16%* and *31%*.

Consequently, it is not possible to set both h_{21} *and* h_{11} *in Hicum equal to the VM approach.*

zoltan.huszka@austriamicrosystems.com

6.2.3 Maximum oscillation frequency, f_{max}

The power dissipated in the epilayer is not encountered for in Hicum. Thus the model is expected to overestimate the ultimate frequency of operation.
It has been shown in [13] that the "passivity function"

$$P_\gamma = \frac{\left|\gamma_{21} + \gamma_{12}^*\right|^2}{4\,\mathrm{Re}(\gamma_{11})\,\mathrm{Re}(\gamma_{22})}$$

goes unity at the same frequency for any sets of the two-port parameters *z*, *y*, *h*, *s* and *g* than the Mason's gain U specifying the unity gain frequency of the transistor. One gets with the *z* parameters of the Hicum approach (right pane of Fig. 4) for the passivity function of the physical equivalent on the left

$$P = \frac{\left|z_{21} + z_{12}^*\right|^2}{4\,\mathrm{Re}(z_{11})\,\mathrm{Re}(z_{22} + rci)} = \frac{\left|z_{21} + z_{12}^*\right|^2}{4\,\mathrm{Re}(z_{11})\,\mathrm{Re}(z_{22})} \frac{1}{1 + \frac{rci}{\mathrm{Re}(z_{22})}}$$

In the vicinity of f_{max} a -20dB/D decline $\left(f/f_{\max}\right)^2$ can be assumed. Since the LHS represents the physical *P*, the Hicum f_{max} can be obtained as

$$f_{\max\_hicum} = f_{\max}\sqrt{1 + \frac{rci}{\Re(z_{22})}} \tag{28}$$

z_{22} is the sum of *re* and the impedance looking in the output of network#1 on the right pane of Fig. 4 with the base node floating. Neglecting *ro* for simplicity and denoting the admittance of *rpi*||*cjc* by *ypi* the voltage *vbei* for an applied output force voltage of *1V* is given as

$$vbei = \frac{s \cdot cjc}{ypi + s \cdot cjc}; \quad s = j\omega$$

The output current results as

$$i = gm\frac{s \cdot cjc}{ypi + s \cdot cjc} + ypi\frac{s \cdot cjc}{ypi + s \cdot cjc}$$

and the output impedance becomes

$$z_{22} = \frac{1}{s \cdot cjc}\frac{ypi + s \cdot cjc}{gm + ypi} + re$$

Note that the intrinsic current gain is

$$h_{21i} = \frac{gm}{ypi}$$

Thus

$$z_{22} = re + \frac{1}{s \cdot cjc}\frac{1}{1 + h_{21i}} + \frac{1}{gm}\frac{h_{21i}}{1 + h_{21i}}$$

Substituting the intrinsic current gain rolloff

$$\frac{1}{h_{21i}} = \frac{1}{h_{21i0}} + \frac{s}{\omega_{Ti}} \approx \frac{s}{\omega_{Ti}}$$

we get

$$z_{22} = re + \left(\frac{1}{\omega_{Ti} cjc} + \frac{1}{gm}\right)\frac{1}{1 + \frac{s}{\omega_{Ti}}}$$

Neglecting *re*

$$\frac{rci}{\Re(z_{22})} = \frac{1+\left(\frac{\omega}{\omega_{Ti}}\right)^2}{1+cf}\omega_{Ti}\cdot\tau_{ci};\quad cf = \frac{\omega_{Ti}\cdot cjc}{gm} = \frac{cjc}{cpi+cjc+gm\cdot\tau_{fi}}$$

Substitution in (28) results

$$f_{\max\_hicum} = f_{\max}\sqrt{\frac{1+cf+2\pi\cdot f_{Ti}\cdot\tau_{ci}}{1+cf-2\pi\cdot f_{Ti}\cdot\tau_{ci}\cdot\left(\frac{f_{\max}}{f_{Ti}}\right)^2}} \tag{29}$$

Assume *cf=0.*2 and as a conservative estimation, $f_{max}=f_{Ti}$. Reading $\tau_{ci} = 0.5ps$ from Fig. 2, the overestimation of f_{max} by Hicum at f_{Ti}=*50GHz* and *100GHz* respectively yields *14%* and *31%*.

7. Summary

I. In recent technologies the contribution of the mobility field dependent base charge term is comparable to the base-Gummel number. This should be addressed in up-to-date compact models like VM and Hicum.

II. Hicum tends to overestimate the transfer current in the quasi/deep saturation range. Bias limits and deviation magnitude are missing from the model documentation.

III. The fact of including τ_{ci} – though formally - in the transit time description should be explicitly stated in the model documentation.

IV. While Hicum describes h_{21} the best among the presently available models it is not possible to set h_{11} concurrently to be equal to that in VM. The process and bias dependent deviation can easily go up to values exceeding 15%. (h_{12} and h_{22} have not been investigated but these are also subject to deviations.)

V. Hicum overestimates f_{max} due to omitting the power dissipated in the epi layer. The error increases with the f_{max}/f_T ratio and can easily exceed 15%.

VI. The inconsistent two-port matrices may lead to unpredictable discrepancies at some AC applications like *rbi* extraction [14] referred to in the Antecedents.

Relocating *rci* to the equivalent – at the cost of an additional (internal collector) node - would eliminate the problems above. Since the bias dependent internal collector resistance is described for the transit time formulation the upgrade might be done even w/o additional model parameters.

zoltan.huszka@austriamicrosystems.com

References

[1] H. K. Gummel, “A Charge Control Relation for Bipolar Transistors,” The Bell System Technical Journal, 1970, pp. 115-120

[2] M. Schroter , H Tran, W. Kraus, “Germanium profile design options for SiGe LEC HBTs,” Solid-State Electronics 48 (2004) 1133–1146

[3] I. E. Getreu, “Modeling the Bipolar Transistor,” Elsevier, 1978

[4] H.K. Gummel and H.C. Poon, "An Integral Charge-Control Model for Bipolar Transistors", Bell Systems Technical Journal, Vol. 49, 1970, pp. 827-852.

[5] M. Schroeter and H. –M. Rein, “A Compact Physical Large Signal Model for High Speed Bipolar Transistors Including the High Current Region,” NTG Meeting, Würtzburg, May 1986.

[6] H. Stübing H.-M. Rein, **„**A compact physical large-signal model for high-speed bipolar transistors at high current densities - Part I: **“,** IEEE Trans. Electron Dev., Vol. 34, pp. 1752-1761, 1987.

[7] M. Schröter, M. Friedrich, and H.-M. Rein, „A generalized Integral Charge-Control Relation and its application to compact models for silicon based HBT's“**,** IEEE Trans. Electron Dev., Vol. 40, pp. 2036-2046, 1993.

[8] H.-M. Rein, H. Stübing and M. Schröter, „Verification of the Integral Charge-Control Relation for High-Speed Bipolar Transistors at High Current Densities,“ IEEE Trans. Electron Dev., Vol. 32, No. 6, pp. 1070-1075, June 1985.

[9] http://www.iee.et.tu-dresden.de/~schroter/Hicum_PD/Hicum22/HICUM-L2V2p2.pdf

[10] M. Schroeter and H. –M. Rein, “Two-Dimensional Modeling of High-speed Bipolar Transistors at High Current Densities Using the Integral Charge-control Relation,” Physica 129B (1985) pp. 332-336

[11] M. Schröter and T.-Y. Lee, „Physics-Based Minority Charge and Transit Time Modeling for Bipolar Transistors“**,** IEEE Trans. Electron Dev., Vol. 46, pp. 288-300, 1999.

[12] M. Malorny, M. Schröter, D. Celi, D. Berger, **“**An improved method for determining the transit time of Si/SiGe bipolar transistors**”,** Proc. BCTM, pp. 229-232, 2003

[13] Z. Huszka, E. Seebacher and K. Molnar, “Estimation of fmax by the Common Intercept Method,” Proc. BCTM, 14.3

[14] Z. Huszka, E. Seebacher and W. Pflanzl, “An Extended Two-Port Method for the Determination of the Base and Emitter Resistance,” IEEE BCTM2005, 11.3

zoltan.huszka@austriamicrosystems.com